UNIWERSYTET JAGIELLOŃSKI W KRAKOWIE
WYDZIAŁ FIZYKI, ASTRONOMII I INFORMATYKI STOSOWANEJ

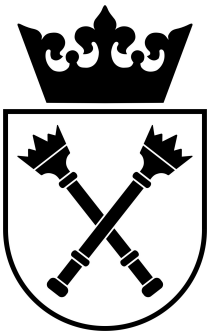

Maria Izabela Lewandowska
Nr albumu: 1136309

Wpływ topologii sieci na rozrost nowotworów

Praca licencjacka
Na kierunku fizyka doświadczalna i teoretyczna

Praca wykonana pod kierunkiem
dr Katarzyny Oleś
Instytut Fizyki

Kraków, 2 July 2019

JAGIELLONIAN UNIVERSITY IN CRACOW
FACULTY OF PHYSICS, ASTRONOMY AND APPLIED COMPUTER SCIENCE

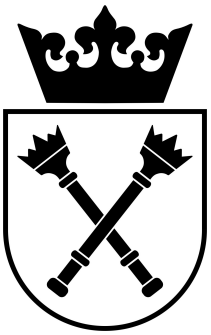

Maria Izabela Lewandowska
Student number: 1136309

The influence of the network structure on tumor growth

Bachelor thesis on a programme
Fizyka doświadczalna i teoretyczna

Prepared under supervision of
dr Katarzyna Oleś
Institute of Physics

Krakow, 2 July 2019

Contents

Abstract

Wykonano ilościową analizę wpływu topologii sieci na rozrost nowotworów. Model namnażania się komórek nowotworowych zastał napisany w oparciu o reakcje kinetyczne modelu Michaelis Menten. Rozrost nowotworu modelowano na dwóch typach sieci: regularnej i małego świata. Skupiono się na zagadnieniach związanych z dynamiką procesu, w szczególności sprawdzono jak parametry modelu (szybkość rozmnażania się komórek nowotworowych, początkowa liczba komórek rakowych oraz koncentracja komórek cytotoksycznych) wpływają na tempo wzrostu guza na sieci regularnej. Ponadto badano wpływ topologii sieci na szybkość namnażania się komórek nowotworowych poprzez analizę pierwszych czasów dojścia (FPT). Uzyskano następujące efekty: szybkość rozrostu nowotworu zależy w głównej mierze od szybkości rozmnażania się komórek nowotworowych oraz koncentracji komórek cytotoksycznych. Początkowa liczba komórek rakowych ma pomijanie mały wpływ. Prawdopodobieństwo zatrzymania rozwoju guza rośnie wraz ze wzrostem koncentracji komórek cytotoksycznych i maleje ze wzrostem szybkości rozmnażania się komórek nowotworowych. Obecność długich linków redukuje czasy dojścia do dowolnie oddalonych fragmentów sieci, czym znacząco zmniejsza odsetek sieci, w których rozwój raka został zatrzymany. W modelu małego świata liczba długich linków jest parametrem dominującym.

Abstract

This quantitative research study was conducted to examine the influence of the network structure on tumor growth. The model of cancer cells' development based on the kinetic reactions of the Michaelis Menten model was modeled on networks: regular and small world. The main focus was on the dynamics of the regular network model, in particular, how different model parameters affect the rate of tumor growth. Analyzed parameters include the rate of tumor cells' proliferation, the initial number of tumor cells and cytotoxic cells' concentration. Based on measurements of first passage times (FTP) the influence of the network structure on the rate of tumor growth was investigated. The following effects have been observed: the rate of tumor growth depends mainly on the cyctotoxic cells' concentration and the rate of tumor cells' proliferation. The influence of the initial number of tumor cells is almost negligible. The probability of stopping cancer development decreases as the cyctotoxic cells' concentration decreases or the rate of tumor cells' proliferation increases. Presence of long range links in the system reduces first passage times and therefore significantly decreases the number of networks, where the cancer development has been inhibited. In small world models, the number of long range links dominates over any other parameter.

Acknowledgements

I would like to thank all the people that helped me prepare the following work.

Foremost, I would like to express my deepest gratitude to my advisor dr Katarzyna Oleś for her continuous support and guidance for the last six months. Similar, profound gratitude goes to prof. Ewa Gutowska Nowak for inspiring my interest in networked systems.

My sincere thanks go to Karol Capała for his invaluable help with struggling with the calculation cluster as well as his innumerable comments.

The following work would not succeed, if not the possibility of performing calculations on the computing cluster shiva.if.uj.edu.pl.

Last by not least, I am grateful to all the people with whom I have had the pleasure to work during the last three years of university studies.

Introduction

The human body consists of trillions of cells grouped to form tissues and organs. Natural life-cycle of each cell is to work, grow, proliferate and finally die. Sometimes this cycle breaks, for example by a gene mutation. Cancer is a disease caused by an uncontrolled division of mutated cells. Cancer cells not only divide out of control and invade nearby tissues, but can also spread to other parts of the organism through the blood and lymphatic system (metastasis).

One approach to investigating cancer growth is to develop a mathematical model. According to [6], the interaction between tumor and immune cells may be formulated in terms of a predator-prey model based on the kinetic reactions of the Michaelis Menten model. An approximate analytical solution of this model is a Langevin type equation describing an overdamped equation of motion in a pseudo-potential in presence of white noise.

An alternative way to examine the given model is to settle it in a networked system. The main objective of this thesis is to examine the influence of the network structure on tumor growth, in particular, to investigate how the presence of long range links changes behaviour of the system.

Quantitative analyze was performed based on measurements of the following quantities:

- range of cancer cells as a function of time in regular network models,
- first passage time in regular network models,
- first passage time in small world models.

This work is organized as follows. In sections 1-3 the historical background is introduced. In sections 4-5 some basic properties of networked systems are recalled. In sections 6-7 is shown problem formulation and implementation. Finally, the results are presented and discussed in sections 8-10 and 11 respectively.

Additionally, in appendix A are presented examples of networks that have been observed during simulations. In appendix B is shown a summary of the percentage of sample networks in which tumor cells reach the given range.

1 Historical background

The early work of Victor Henri (1903) on the kinetics of the invertase-catalysed reaction showed that the rate of inversion is proportional to the amount of invertin [1].

$$\text{Initial\_rate} = \frac{K_3 \cdot a}{1 + m \cdot a} \tag{1.1}$$

where a is the amount of sucrose (substrate), K_3 is a constant proportional to the ferment (enzyme) concentration and m is an equilibrium constant.

Henri's study was the starting point for Michaelis and Menten work. In 1903 in the famous paper [2] they introduced a mathematical model of enzymatic reaction that binds enzyme (E) to a substrate (S) forming a complex (SE) which breaks down into a glucose (G) and fructose (F) regenerating the original enzyme:

$$\text{Sucrose} \xrightarrow{\text{Invertase}} \text{Fructose} + \text{Glucose}$$

$$\text{E} + \text{S} \overset{\text{K}_\text{S}}{\rightleftarrows} \text{SE} \xrightarrow{c} \text{E} + \text{F} + \text{G} \tag{1.2}$$

In the expression above K_s is a equilibrium dissociation constant for sucrose. The total amount of enzyme is constant over time:

$$\text{E} + \text{SE} = const \tag{1.3}$$

The rate of the reaction is proportional to the concentration of the complex:

$$v = \frac{d[G]}{dt} = \frac{d[F]}{dt} = c \cdot [ES] \tag{1.4}$$

The initial velocity v_0 of the reaction under the assumption that the initial stage of the complex SE formation is very fast, and at equilibrium is equal to zero, is equal to:

$$v_0 = V_{max} \frac{[S]}{[S] + K_M} \tag{1.5}$$

V_{max} - the maximum rate of the reaction achieved at saturating point of substrate concentration, K_M - Michaelis constant.

Equation (1.5) is known as Michaelis and Menten equation [4]. Estimate value of K_M was derived from experimental data by the authors. Michaelis Manten work was confirmed and developed by many scientists over the last hundred years.

2 Basic enzyme reactions

Although Michaelis Manten equation was initially a mathematical model for invertase only, it may be applied to many different enzyme kinetics reactions [3]. invertaseIf we put E, S, SE and P as enzyme, substrate, complex and product respectively, we obtain a generalization of (1.2):

$$\mathrm{E} + \mathrm{S} \underset{\mathrm{k}_{-1}}{\overset{\mathrm{k}_1}{\rightleftarrows}} \mathrm{SE} \xrightarrow{k_2} \mathrm{P} + \mathrm{E} \tag{2.1}$$

where $k_1, k_{-1}, k_2 > 0$ are constant parameters associated with the rates of reaction.

According to the law of mass action, the rate of reaction is proportional to the product of the active masses of reactants. If we set:

$$s = [S], \qquad e = [E], \qquad z = [SE], \qquad p = [P] \tag{2.2}$$

as concentration of subtract, enzyme, complex and product respectively, from (2.1) we obtain a set of four linear first order differential equations:

$$\begin{aligned} \frac{ds}{dt} &= -k_1 \cdot s \cdot e + k_{-1} z \\ \frac{de}{dt} &= -k_1 \cdot s \cdot e + (k_{-1} + k_2)\, z \\ \frac{dz}{dt} &= k_1 \cdot s \cdot e - (k_{-1} + k_2)\, z \\ \frac{dp}{dt} &= k_2 \cdot z \end{aligned} \tag{2.3}$$

The initial conditions are given by the physical process of the reaction:

$$s(0) = s_0 \qquad e(0) = e_0, \qquad z(0) = 0, \qquad p(0) = (0). \tag{2.4}$$

There is no analytical solution of (2.3) if we want to meet the initial conditions (2.4). An interesting approach to the problem was broadly discussed in the literature [5].

3 The model of tumor growth

The mathematical model provided by Michaelis and Manten might be also used to describe the dynamics of interacting populations. According to [6] an approximation of local interaction between tumor and cytotoxic cells may be given by the catalytic Michaelis-Menten scenario (3.1). Cytotoxic cells Y and cancer cells X bind together at rate k_1 to form a complex Z. The complex decays at a rate k_2 to a dead cell P regenerating the original cytotoxic cell. In addition to that, cancer cells may proliferate spontaneously at a rate λ. The model system is given by the reaction scheme (3.1).

$$\begin{gathered} \mathrm{X} + \mathrm{Y} \xrightarrow{k_1} \mathrm{Z} \xrightarrow{k_2} \mathrm{Y} + \mathrm{P} \\ \mathrm{X} \xrightarrow{\lambda} 2\mathrm{X} \end{gathered} \tag{3.1}$$

Analogically as in the previous section, the reaction might be expressed in terms of cells' concentration:

$$x = [X], \qquad y = [Y], \qquad z = [Z], \qquad p = [P] \tag{3.2}$$

where x, y, z, p stand for the concentration of cancer, cytotoxic, complex and dead cells respectively. The dynamics of the model is now given by a set of first order differential equations:

$$\begin{aligned}
\frac{dx}{dt} &= \lambda \cdot x - k_1 \cdot x \cdot y \\
\frac{dy}{dt} &= -k_1 \cdot x \cdot y + k_2 \cdot z \\
\frac{dz}{dt} &= k_1 \cdot x \cdot y - k_2 \cdot z \\
\frac{dp}{dt} &= k_2 \cdot z
\end{aligned} \tag{3.3}$$

Typical values of the parameters k_1, k_2 and λ are: $k_1 \in (0.1, 18)\left[\frac{1}{\text{day}}\right]$, $k_2 \in (0.2, 18)\left[\frac{1}{\text{day}}\right]$, $\lambda \in (0.2, 1.5)\left[\frac{1}{\text{day}}\right]$ [6]. Sample solutions of (3.3) are shown in figure 3.1:

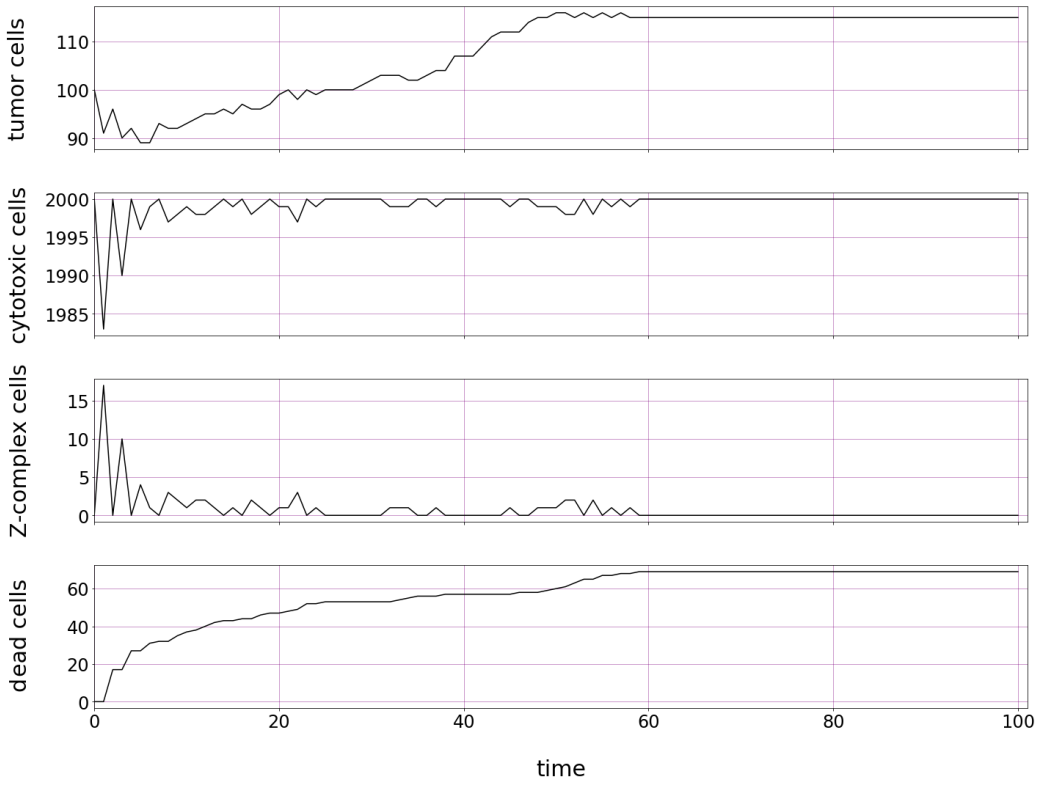

Figure 3.1: Behaviour of the solutions of (3.3) for the tumor, cytotoxic, z-complex and dead cells' concentrations as functions of time. Simulation parameters: $\lambda = 1.0$, $k_1 = 1$, $k_2 = 1$, cytotoxic cells' concentration: $c = 0.2$, initial number of tumor cells: $X_{init} = 100$. Network size: 100×100.

4 Network systems

A network is a set of vertices (nodes) connected to one another by edges. A convenient representation of a networked system is a graph, see fig. 4.1. There are many kinds of real systems that may take a form of networks, for example, World Wide Web, social networking services or biological interactions [7]. In particular, a biological system might be represented as a network of physical interactions between its elements. Network models are irreplaceable when we want to predict the behavior of the system based on its structural properties and the local rules governing individual vertices [7].

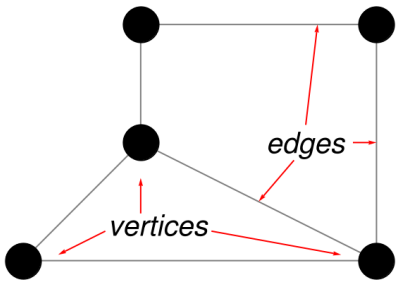

Figure 4.1: A graph with five vertices and six edges.

Most of the mentioned systems are too large and sophisticated to analyze properties of individual vertices or edges. Instead, we put under consideration the statistical properties of the network (degree distributions, transitivity, network resilience [7]), that characterise its structure and behaviour.

Once the solution for a network model is found, it may be applied to various systems described by the same model. Consequently, we may put away the physical properties of the system and focus on characteristic features of the networked one.

Studying networked models, one could find similarities in topology and behaviour in networks that describe completely different physical systems. In particular, we may distinguish the following three types of network:

- regular networks
- scale-free networks
- small world networks
- random graphs

Scale-free networks are networks with power-law degree distributions [8]:

$$P(k) \sim k^{-\gamma} \tag{4.1}$$

where $P(k)$ is probability that the given node have k connections to other nodes, γ is a constant parameter.

In random graphs are networks where randomly chosen vertices are connected by undirect edges. Regulat and small world networks will be discussed in the next two subsections.

4.1 Regular network

The regular network is a highly ordered graph whose drawing is embedded in a n-dimensional Euclidean space. The number of edges that connect each vertex to its k closest neighbors (known as the coordination number z) in regular networks is the same for each node. Examples of regular networks in one, two and three dimensions are shown on figures 4.3a and 4.2 respectively.

Due to the geometrical properties, in regular networks, the mean geodesic distance between vertex pairs is relatively high.

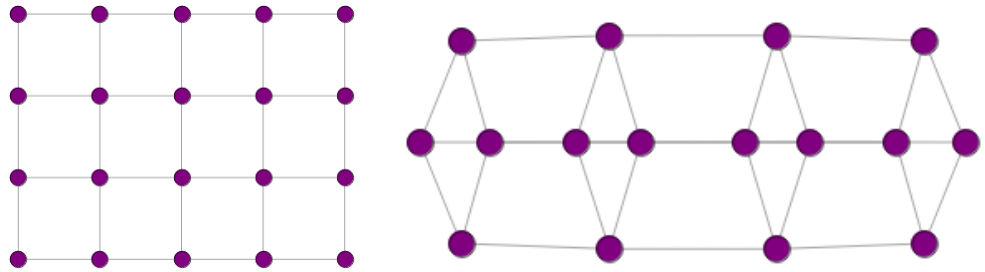

(a) (b)

Figure 4.2: Regular network in a) two dimensional ($z_{2D} = 4$) and b) three dimensional ($z_{3D} = 6$) Euclidean space.

4.2 Small world model

Small world model arises from a low dimensional regular network when a small fraction of 'shortcuts' (long range links) is added. Those 'shortcuts' result from moving regular edges or adding a new one under condition that no double edges or self-edges are allowed. Long range links between any two verticals are equally probable.

In [7] two different ways of obtaining a small world network were discussed:

- rewiring existing edges so that with probability p one end of each edge is moved to a new vertex randomly chosen from the lattice, see fig. 4.3b. The network after rewiring procedure consist of the same number of edges as the original one. The average coordination number z remains constant as well.

- adding new edges between two randomly chosen verticals, see fig. 4.3c. Probability per edge p that long range links occur anywhere in the network has similar meaning like the probability defined in the previous procedure. Both the number of edges and the average coordination number z changes.

In both cases, for $p = 1$ small world model behaves similar to a random graph, for $p = 0$ the model is a regular network with all its geometrical and statistical properties.

Small world models are characterised by high transitivity and low path lengths (mean geodesic distance between vertex pairs in a network) [7]. Those two factor simply that the spread of information in small world models is faster than in regular ones.

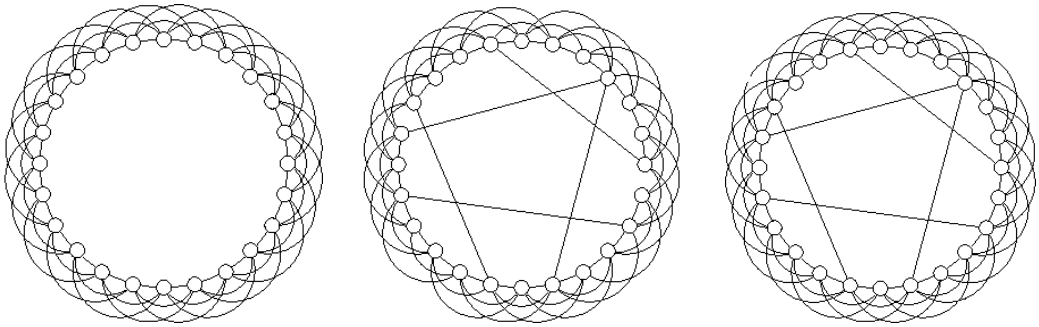

(a) (b) (c)

Figure 4.3: (a) A one-dimensional lattice with connections between all vertex pairs separated by three lattice spacing. (b) The small-world model created by choosing at random a fraction of the edges in the graph and moving one end of each to a new, randomly chosen location. (c) The small-world model created by adding shortcuts between randomly chosen vertices. Source: [7].

5 First passage time

The main practical problem one confronts studying networked systems is finding a convenient way of describing passage properties in a network.

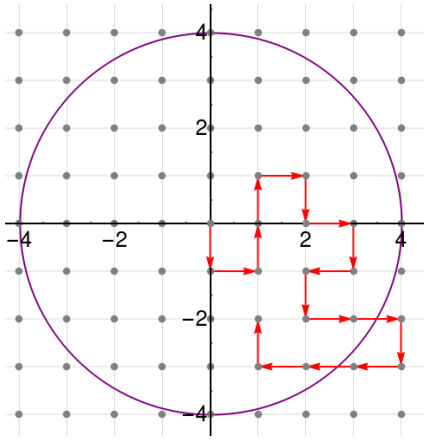

Figure 5.1: Random walk in a two-dimensional Euclidean lattice.

Even if we know explicitly the geometrical structure of the network (network dimension, the average number of nodes, type of interaction), it is difficult to predict how fast the signal propagate due to its probabilistic nature.

To get a better picture, we could imagine a random walk in a two-dimensional Euclidean lattice, see fig. 5.1. Starting from the point $\vec{r}_0 = (0,0)$ the walker goes one step at a time Δt in a randomly chosen direction (left, right, up, down). No direction is privileged.

From the general theory of Markov chains one could figure out the probability density $W(\vec{r},t|\vec{r}_0)$ that the walker is at position $\vec{r}$ at time t. But sometimes we are not interested in where the walker is right now, but how long it took to reach a given target point. Let $P(\vec{r},t|\vec{r}_0)$ be the probability density that the walker reaches for the first time a given position $\vec{r}$ at a specified time. $W(\vec{r},t|\vec{r}_0)$ and $P(\vec{r},t|\vec{r}_0)$ are related as shown below [10]:

$$W(\vec{r},t|\vec{r}_0) = \int_0^t P(\vec{r},\tau|\vec{r}_0)W(\vec{r},t-\tau|\vec{r}_0)d\tau \tag{5.1}$$

In case of discrete time domain the relation (5.1) could be written as:

$$W(\vec{r}, n|\vec{r}_0) = \sum_{n'=0}^{n} P(\vec{r}, n'|\vec{r}_0) W(\vec{r}, n-n'|\vec{r}_0) \tag{5.2}$$

$P(\vec{r}, t|\vec{r}_0)$ is known as first passage time (FPT). In case of networked systems, FPT is a quantity that measure the time needed to reach selected node (set of nodes) starting form the initial node. In multidimensional networks FPT is usually characterised by the exit time from a (hiper)sphere (the first time a random walker reaches any point at a distance r from its starting point [9][10].

The explicit relation between the FPT and the structural properties of a network is difficult to achieve as both $W(\vec{r}, t|\vec{r}_0)$ and $P(\vec{r}, t|\vec{r}_0)$ depend on the walk's characteristics and the domain in which the walk is performed. Over the last few decades, an extensive literature has developed on passage properties [9], [10], [11], however, first passage time phenomena is still an open question.

6 Problem formulation

To obtain a rough picture of the behavior of the system described by (3.1), we may reformulate the model in terms of a networked system and apply it to simulate evolution of cancer. In a graph representation the network is in the form of two-dimensional Euclidean lattice, see fig 6.1. Each node represents a cell (tumor, cytotoxic, complex or dead cell) while edges stands for connections between cells.

The fundamental assumptions of the model are as follows:

- evolution of the model is given by (3.1),
- the model is settle in a discrete time-space domain,
- the size of the lattice is constant and finite: $\text{size}_\text{x} = \text{size}_\text{y} = 100$,
- border effects are neglected,
- present state of the network depends only on its state in the previous iteration,
- cytotoxic and tumor cells interact only with their direct neighbourhood (four cells). If there are long range links in the system (small world effect) this number for tumor cells could be increased to five at maximum,
- to preserve system memory, instead of Z complex cells we have ZX and ZY complex that 'remember' their past state as X or Y cell,
- dead cells don't interact and are removed from the system after one iteration,
- first passage time is defined as the number of iteration in which cancer cells cross the border of the sphere with radius r and center coincident with the center of the lattice.

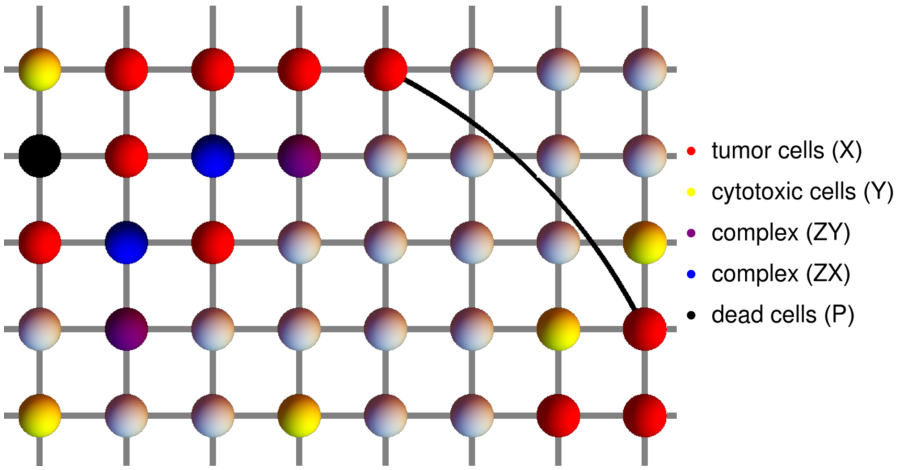

Figure 6.1: Graph representation of the model system (3.1). Red, yellow, blue, purple and black circles stand for tumor, cytotoxic, ZX-complex, ZY-complex and dead cells respectively.The long range links are shown as black curves while short range links are shown as grey lines.

After defining the structure of the network, we may proceed with quantitative analysis of the model. The aims are twofold: First to examine the regular network model, including the influence of parameters c, λ, X_{init} on model evolution, second to check the impact of network topology on changes in first passage time.

7 Implementation

7.1 Initial conditions

Initial conditions of the network are defined as follows: The cancer cells are arranged according to two dimensional Gauss (for $X_{init} = 50$) or Laplace (for $X_{init} = 100$) distribution. Scaling parameters in both distributions were chosen so that the initial shape of tumor was spherical. Cytotoxic cells are randomly distributed in the remaining free space. Cytotoxic cells can not have long links connections. In case of small world systems, n_{links} pairs of randomly chosen cells are connected using long range links.

7.2 Program

Measurements of the range of tumor were performed using the program simulating the evolution of the network described by the model. The program works as follows: For the given input parameters, k sample networks are simulated, $n = 5000$ iteration each. Final results are saved to two csv files:

1. list of ranges of tumor at the moment of simulation termination
2. table (k rows, 7 columns) of first time passages for $r = \{0, 5, 10, 20, 30, 40, 50\}$.

Each file has a header containing all necessary information about simulation parameters. The simulation stops when one of the following conditions is fulfilled:

- the range of tumor cell cluster reach the border of the network
- the specified number of iteration n has been executed

The main program consists of Graphical User Interface (GUI), see fig. 7.1 and two functions:

- *run simulation()* - run k simulations with the same entry parameters and save the results to csv file. All the parameters are taken from GUI.
- *single network diagnosis()* - run simulation for a single network to get a full history of the network evolution, including network picture after each iteration. The parameters for the network are taken from GUI.

The program was written in Python using libraries: numpy, pandas, deepcopy, sys, math and time [1]. Data visualization was done using the matplotlib.pyplot environment. Graphical User Interface, see fig. 7.1, was made in Jupyter notebook using IPython.display and ipywidgets libraries.

The chosen method has potential limitations related to the computing power. The size of the network can not be to big and there are strong restrictions for number of iterations as each iteration requires checking ($\text{size}_\text{x} \times \text{size}_\text{y}$) cells.

7.3 Simulation parameters

In the further part of this work the concentration of cytotoxic cells is represented as c instead of y. The number of cytotoxic cells is given by (7.1).

$$Y = c \cdot \text{size}_\text{x} \cdot \text{size}_\text{y} \tag{7.1}$$

Parameters $k_1 = k_2 = 1$ are static. The dynamic parameters of the model are shown below:

- $\lambda = \{0.3, 1.0\}$ - rate of tumor cells proliferation
- $c = \{0.1, 0.15, 0.2\}$ - cytotoxic cells concentration
- $X_{init} = \{50, 100\}$ - initial number of tumor cells
- $n_{links} = \{25, 50, 100, 200\}$ - number of long range links in the system

[1] For interested readers the program, as well as complete data from simulation, are available at github repository: `https://github.com/Milwa97/Bachelor`

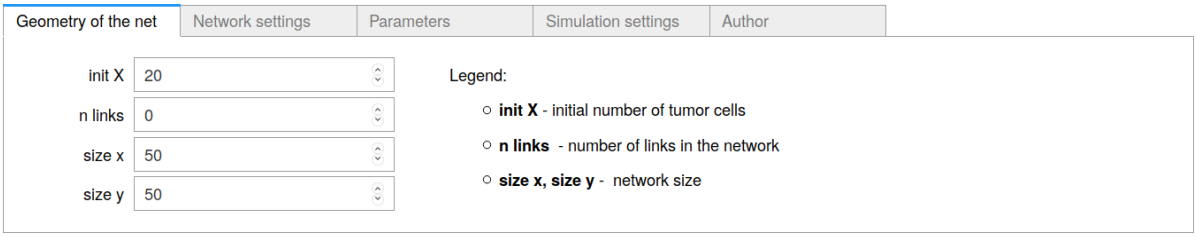

(a) Geometry of the net panel

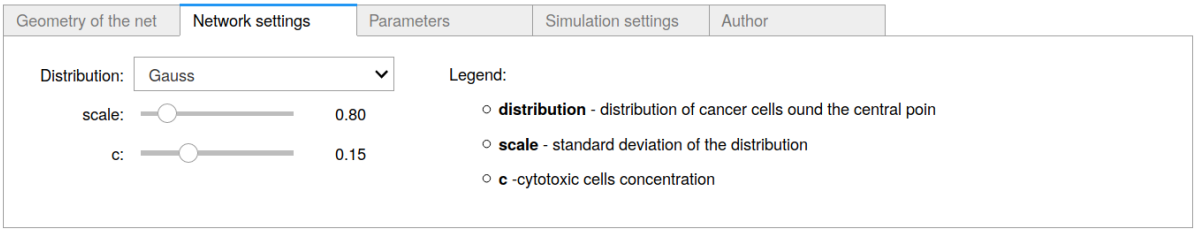

(b) Network settings panel

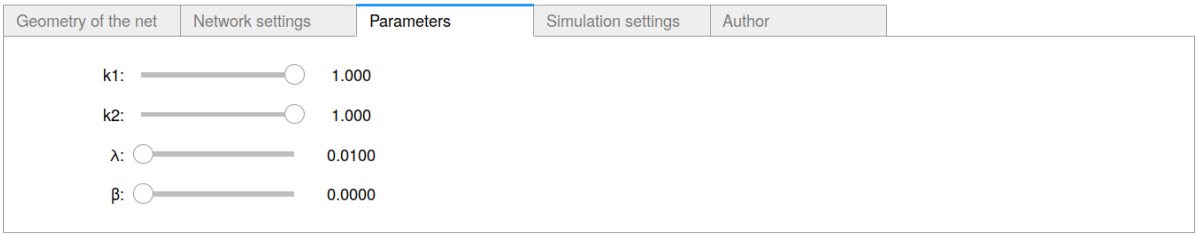

(c) Network parameters panel

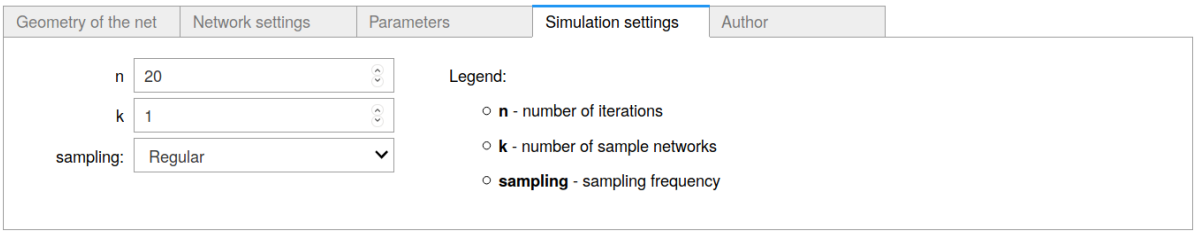

(d) Simulation settings panel

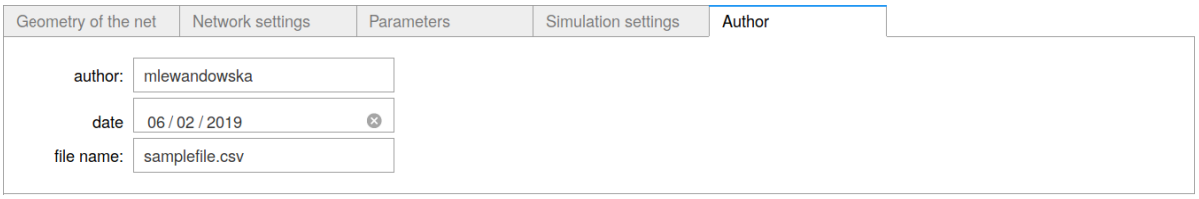

(e) Author and file options panel

Figure 7.1: Graphical user interface.

8 Results

Qualitative analysis was based on data collected from simulations: $k = 100$ and $k = 200$ samples for each set of input parameters in case of regular and small world networks respectively. Main focus was to discover the dynamics of the process by measuring the impact of model parameters, e.g. λ, c, X_{init} and n_{links} and examine for which values of parameters λ, c, X_{init} the development of tumor cells was stopped. The first passage times were measured for two different network structures: regular network and small world.

9 Regular network

9.1 The influence of rate of tumor cells proliferation on tumor growth

For small values of λ parameter ($\lambda = 0.3$) the tumor development stops completely within the first 500 iterations. For $\lambda = 1.0$ tumor cells spread over the entire the available area in a very short time, see fig. 9.1. Based on figure 9.2 it is clear that for a regular network the λ parameter plays a key role.

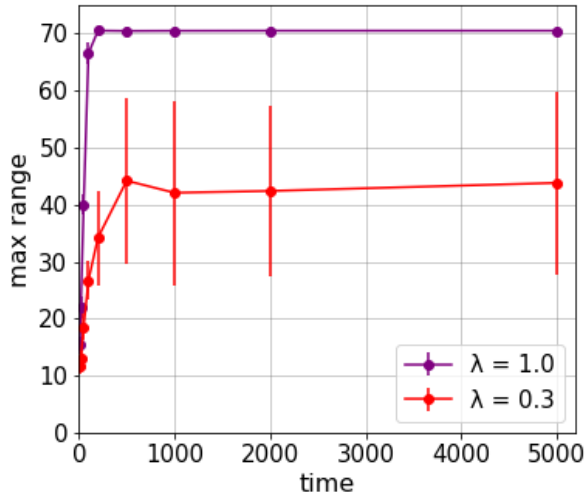

Figure 9.1: The range of tumor as a function of time for different values of λ parameter. Other simulation parameters: initial number of tumor cells: $X_{init} = 50$, cytotoxic cells' concentration: $c = 0.15$. Error bars are given by a normalised standard deviation.

9.2 The influence of cytotoxic cell' concentration on tumor growth

A significant contribution to the rate of cancer development is made by cytotoxic cells' concentration. As the concentration decrease, the chance of stopping the development of cancer decrease too, see Tables 11.1, 11.2. Moreover, cytotoxic cells' concentration has a big impact on the shape of the cancer cells' cluster: for low concentration ($c = 0.10$) the shape of the cluster is spherical. In case of high cytotoxic cells' concentration ($c = 20$) shape of the cluster is very uneven. For low cytotoxic cells' concentration the influence of λ parameter is negligibly small, see fig. 9.2 and Tables 11.1, 11.2.

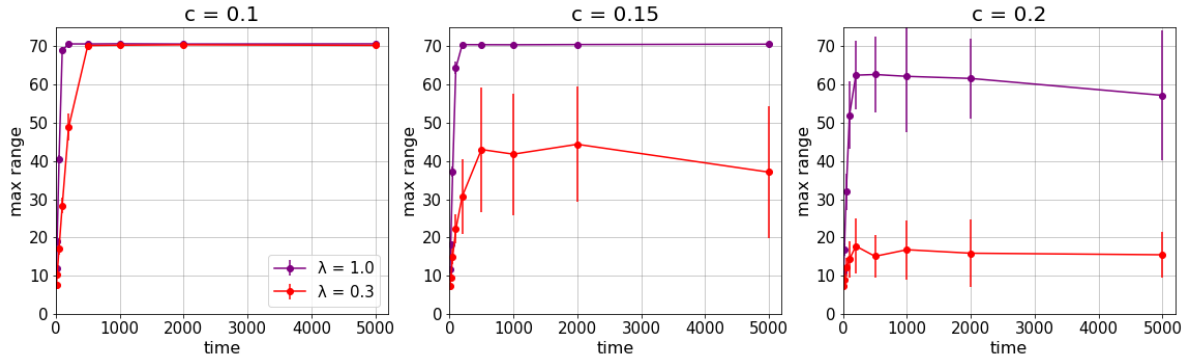

Figure 9.2: The range of tumor as a function of time for different values of cytotoxic cells' concentration. Other simulation parameters: initial number of tumor cells: $X_{init} = 50$. Error bars are given by a normalised standard deviation.

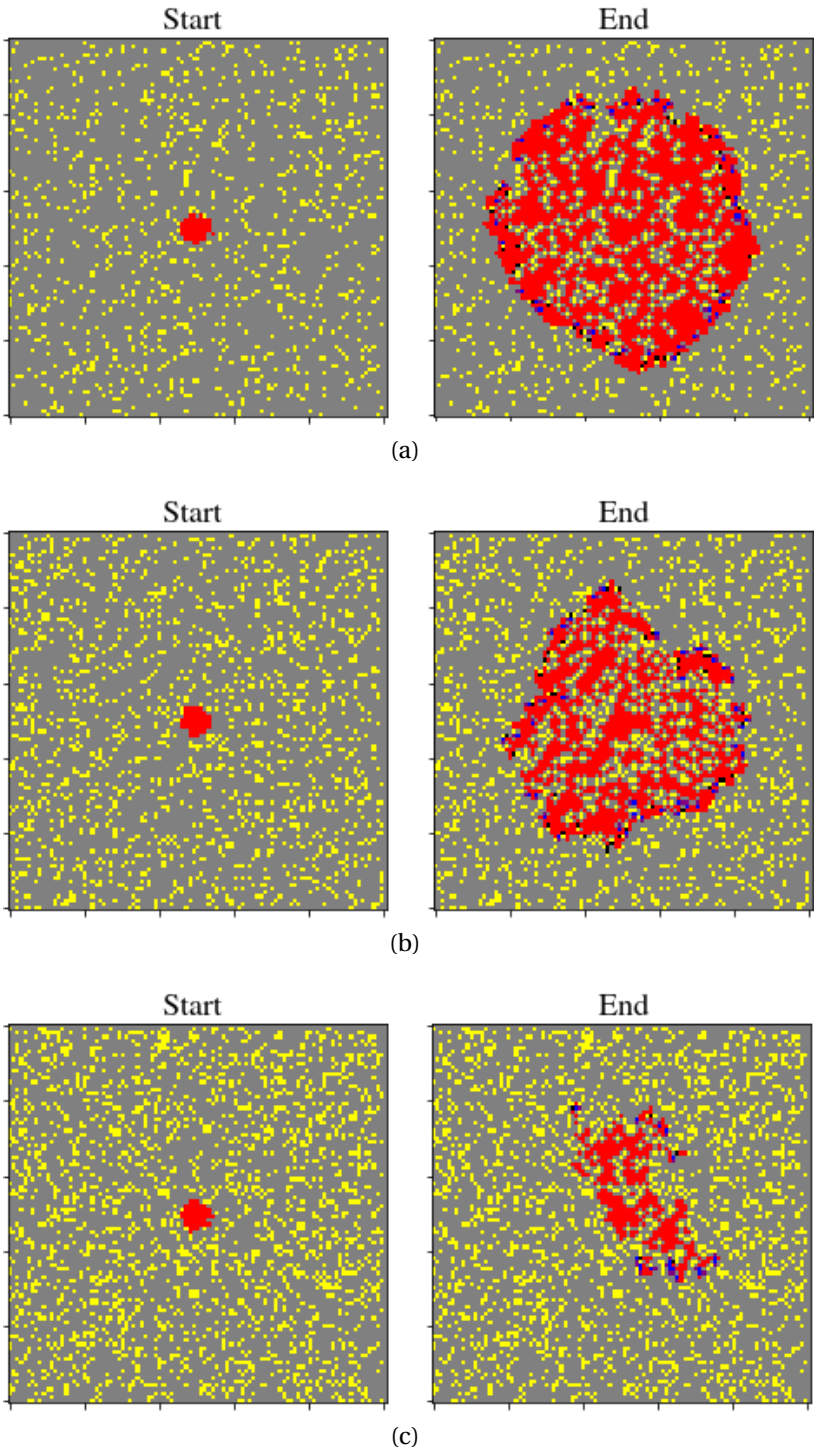

Figure 9.3: The evolution of the cancer for different values of cytotoxic cells' concentration: $c = 0.10$ (top), $c = 0.15$ (centre), 0.20 (bottom). Other simulation parameters: rate of tumor cells' proliferation: $\lambda = 1.0$, initial number ot tumor cells: $X_{init} = 50$, number of iterations: $n = 50$. Red, yellow, blue, purple and black points stand for tumor, cytotoxic, ZX-complex, ZY-complex and dead cells respectively.

9.3 The influence of the initial number of tumor cells on tumor growth

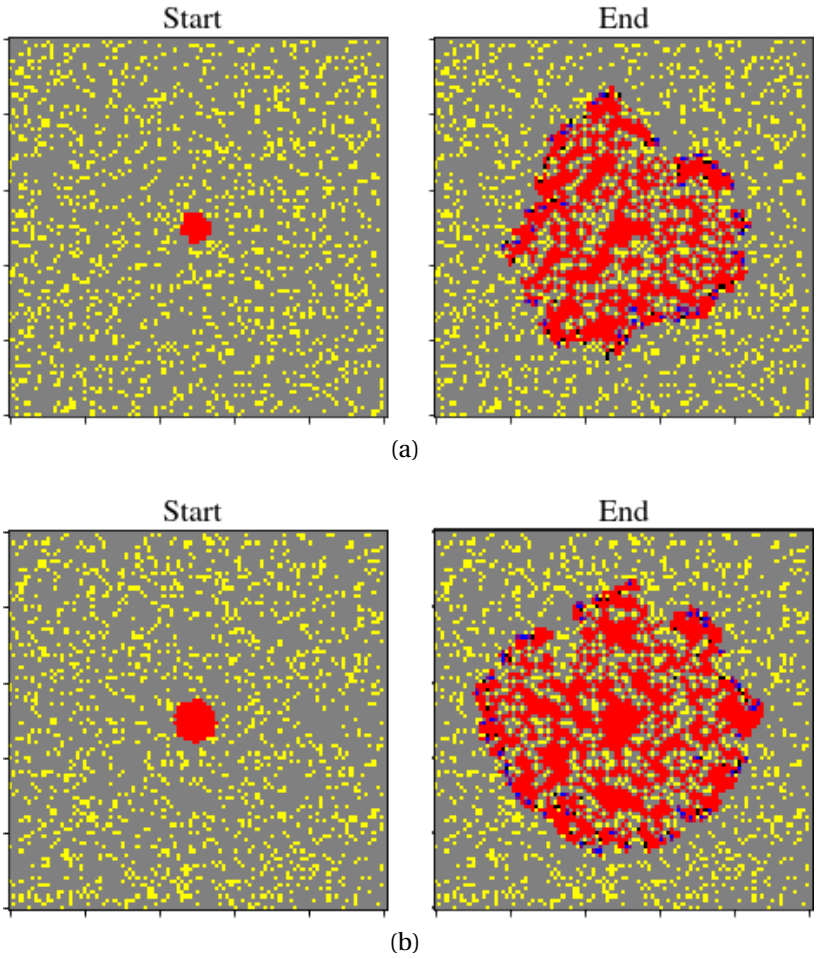

Figure 9.4: The evolution of the cancer for different initial number of tumor cells: $X_{init} = 50$ (top), $X_{init} = 100$ (bottom). Other simulation parameters: rate of tumor cells' proliferation: $\lambda = 1.0$, cytotoxic cells' concentration: $c = 0.15$, number of iterations: $n = 50$. Red, yellow, blue, purple and black points stand for tumor, cytotoxic, ZX-complex, ZY-complex and dead cells respectively.

Initial number of tumor cells has a small influence on system evolution. Based on figures 11.2a, 11.1a we observe that the highest expansion rate of tumor cells is at the beginning of the simulation. If the development of cancer has not been stopped at an early stage, it does not matter after all, what the initial number of tumor cells was. Only for small λ values the probability of stopping cancer development for $X_{init} = 50$ is greater than for $X_{init} = 100$, but . For $\lambda = 1.0$ no significant difference was observed, see Tables 11.1, 11.2.

10 Influence of network topology on first passage time

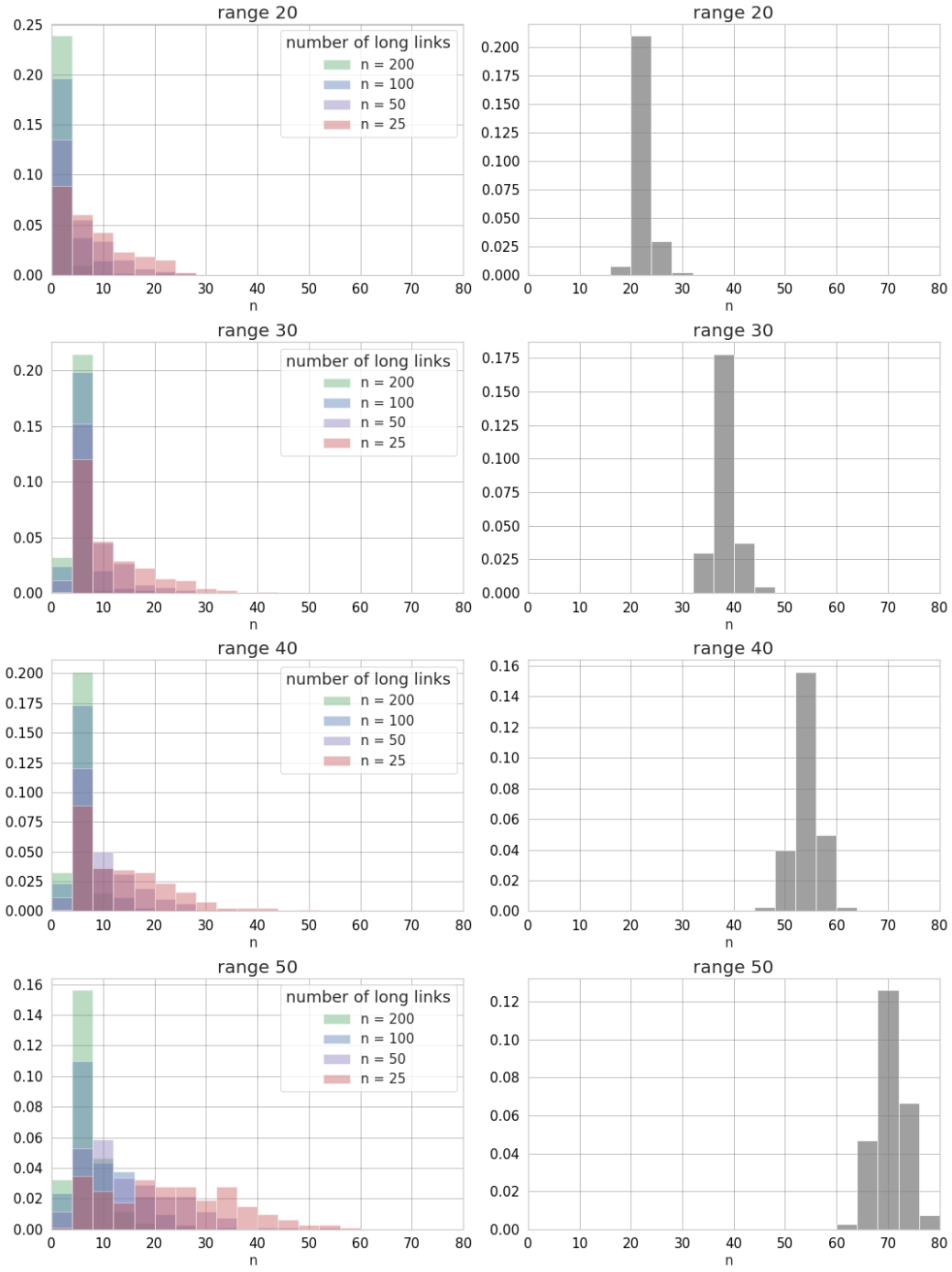

Figure 10.1: First time passage distribution in a small world model for different numbers of long range links in the system (left) and for a regular network (right). Other simulation parameters: rate of tumor cells' proliferation: $\lambda = 1.0$, initial number of tumor cells: $X_{init} = 50$, cytotoxic cells' concentration: $c = 0.15$.

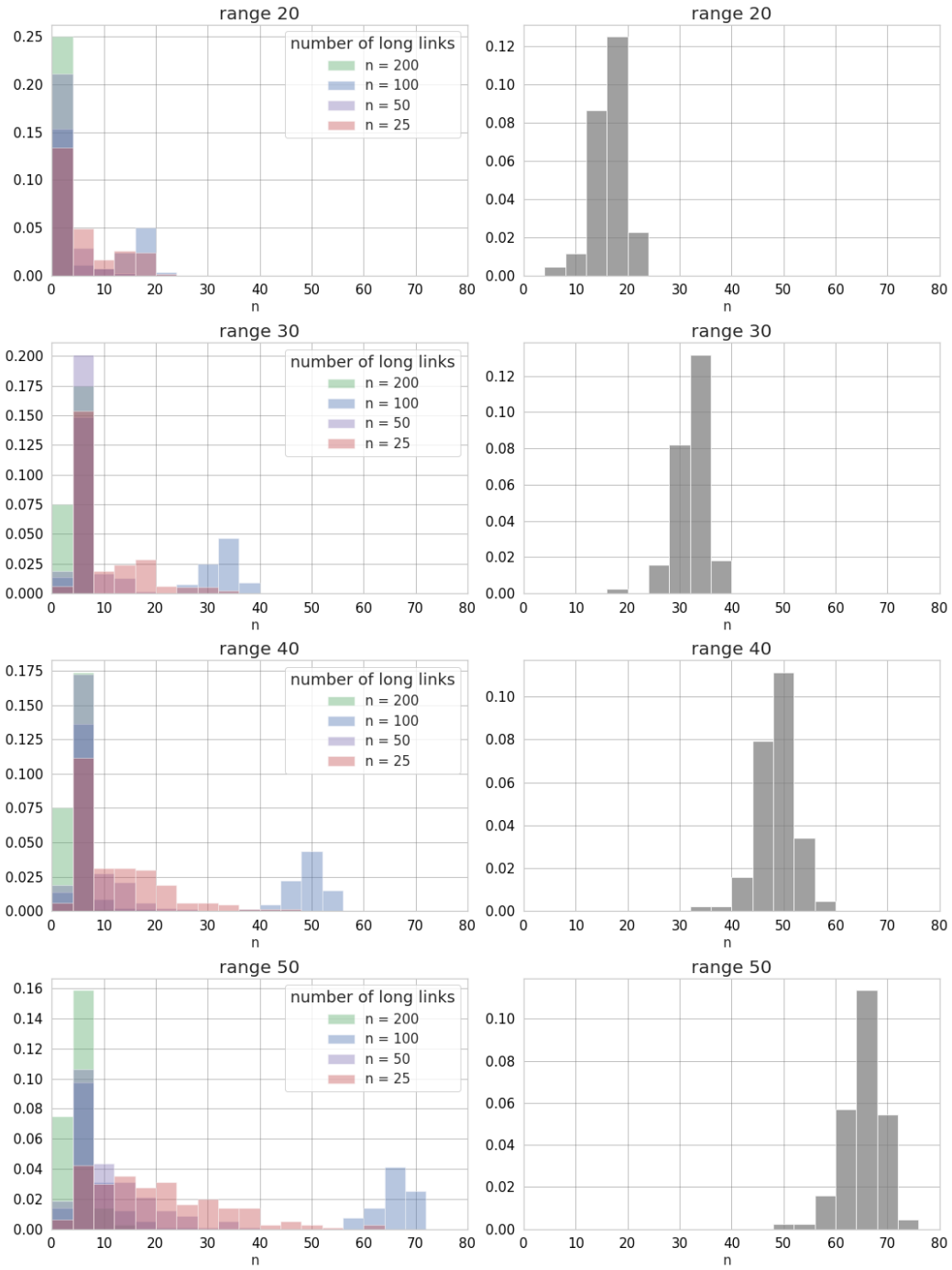

Figure 10.2: First time passage distribution in a small world model for different numbers of long range links in the system (left) and for a regular network (right). Other simulation parameters: rate of tumor cells' proliferation: $\lambda = 1.0$, itial number of tumor cells: $X_{init} = 100$, cytotoxic cells' concentration: $c = 0.15$.

Two different network structures were examined. First time passage was computed in order to discover the impact of network type on tumor growth.

Figures 10.1, 10.2 show distributions of first time passages for different values of X_{init} and c parameters.

In case of regular network the main peak moves as the range of tumor increases. The further the cancer expands, the longer it takes. The peaks width increases with time, n. What is more, as cytotoxic cells concentration increases, the number of iteration needed for cancer to reach a given range increases too. Those effects are quite obvious, as the range of tumor cells is a monotonically increasing function of time, n and cytotoxic cells concentration, c, see fig. 9.4a, 9.4b. In comparison to small world model, first time passage for any chosen range is centred around the first few iterations.

Noteworthy is the occurrence of two peaks in for small model network, see fig. 10.1. The first peak is caused by the presence of long range links in the system, while the second, smaller one occurs in smaple networks, where was no 'jumps' through long connections. The second peak act the same way as the main peak in regular network models. The first peak corresponds to the occurrence of metastatics, whereas the second one corresponds to the tumor that growths locally.

We could expect that the ratio of the height of the first and second peaks should be proportional to the total number of long range links in the system, however, it has not been observed. For small world model only a fraction of all sample networks reach ranges $r = \{20, 30, 40, 50\}$, see Tables 11.3, 11.4, 11.5, 11.6, 11.7, 11.8, therefore the second peak is significantly lower. Due to histogram normalisation, this phenomena is unnoticeable on regular network charts.

In appandix B the influence of parameters λ, X_{init}, c, n_{links} on percentage η of sample networks where tumor cells reach the given range $r = \{20, 30, 40, 50\}$ is shown. The data implies that for $\lambda = 1.0$ η is always greater than for $\lambda = 0.3$. In a small world models η is substantially greater than in a regular network, however, even for a relatively large number of long range links in the small model system ($n_{links} = 100$, $n_{links} = 200$) η is not equal to 100%, see Tables 11.7, 11.8, 11.9, 11.10.

11 Conclusion

The results confirm that the network topology substantially affects the first time passages as well as on the percentage of sample networks where tumor cells' development have been stopped. The measurable effects related to the presence of long range links in the system are:

- significant reduction of the first passage times, see figures 10.1, 10.2
- decreasing number of networks, where the cancer development is inhibited, see Tables 11.1, 11.2, 11.3, 11.4, 11.5, 11.6, 11.7, 11.8, 11.9 11.10

It has also been discovered that the number of long range links dominates over any other parameter in small world models.

The results provide a basis for further research. In particular, in case of regular network the following issues remain open:

- What is combined total impact of k_1, k_2 and λ parameters on the system behaviour? How those parameters depend on each other?
- Is the system scalable ? How the range of cancer cells changes if there is no limit to the size of the network?
- How the system would behaviour in three dimension ?
- Which parameters determine the inhibition of network development? Is there any hyperplane in parameter space (k_1, k_2, λ, c) that would separate fully developed network from the inhibited ones?

References

[1] V. Henri, *Lois Générales de l'action des Diastases*, Librairie Scientifique A. Hermann, (1903)

[2] L. Michaelis, M. Menten, *Die Kinetik der Invertinwirkung*, iochemische Zeitschrift 49:333–369 (1913)

[3] Ch. M. Hill, R. D. Waight, W. G. Bardsley, *Does any enzyme follow the Michaelis-Manten equation?*, 15 Volume, Springer (1977)

[4] K. A. Johnson, R. S. Goody, *The Original Michaelis Constant: Translation of the 1913 Michaelis-Menten Paper*, Biochemistry (2011)

[5] J.D Murray, Mathematical Biology: I. An Introduction, Third Edition, 17 Volume, Springer (2002)

[6] A. Fiasconaro, A. Ochab–Marcinek , B. Spagnolo, E. Gudowska–Nowak, Monitoring noise-resonant effects in cancer growth influenced by external fluctuations and periodic treatment, Eur. Phys. J. B65, 435–442 (2008)

[7] M.E.J. Newman, The structure and function of complex networks, 45 Volume, SIAM Review (2003)

[8] A. Barabási, R. Albert, *Emergence of scaling in random networks*, VOL 286, Science (1999)

[9] S. Redner, *A Guide to, First-Passage Processes*, Cambridge University Press (2001)

[10] S. Condamin, O.Benichou, V. Tejedor, R. Voituriez1, J. Klafter, *First-passage times in complex scale-invariant media*, Vol 450|1 nature, (2007)

[11] H. W. Lau, K. Y. Szeto, *Asymptotic analysis of first passage time in complex network*, 90, EPL, (2010)

Appendix B: Figures

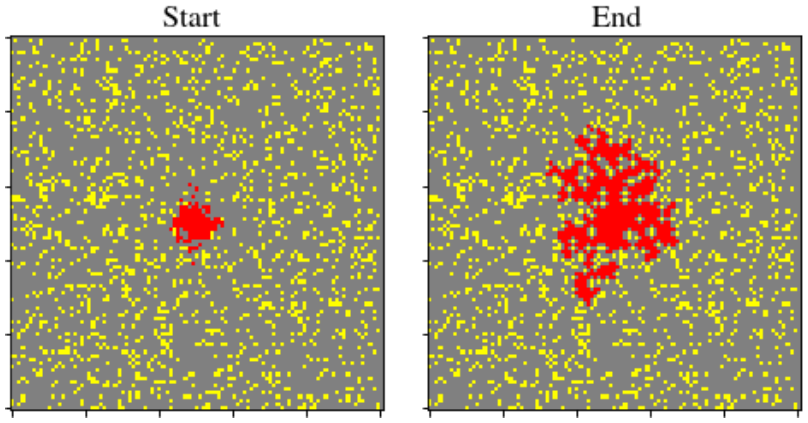

(a)

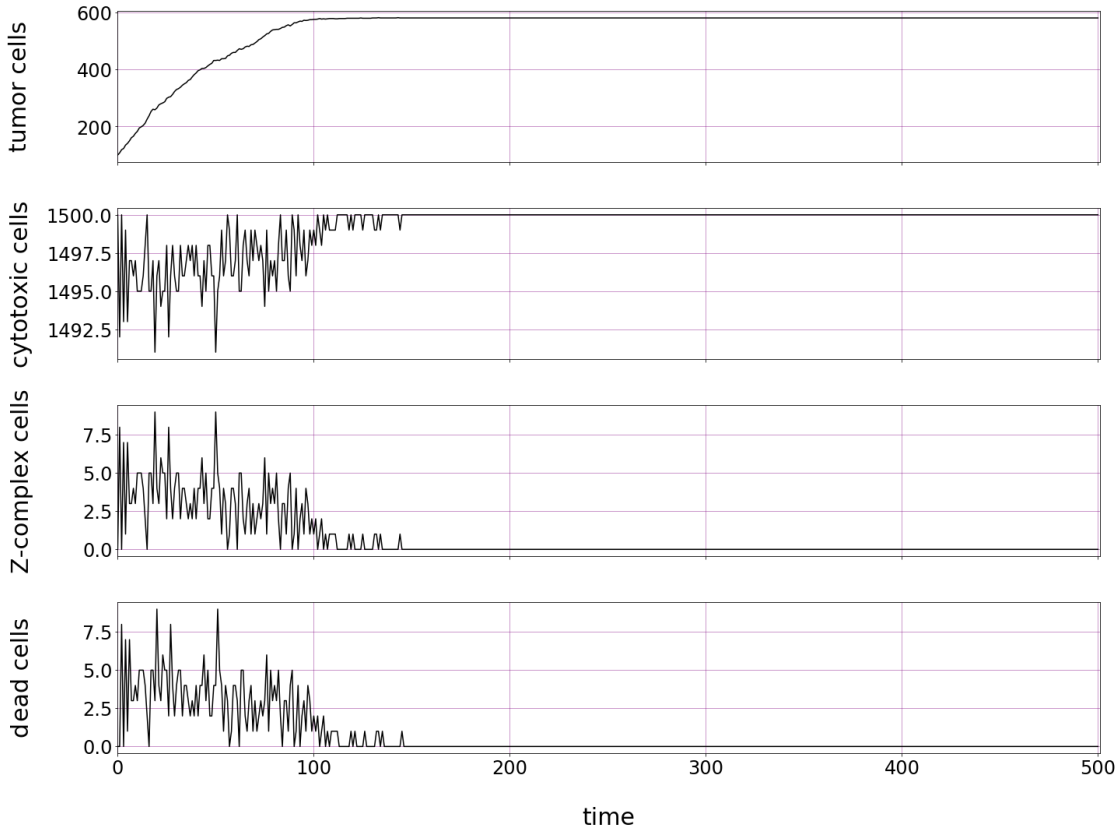

(b)

Figure 11.1: The evolution of the tumor that leads to tumor inhibition in a lattice model a) initial state (left) versus state after $n = 500$ iterations (right), b) changes in concentration of tumor, cytotoxic, Z-complex and dead cells as a function of time. Simulation parameters: $\lambda = 0.3$, $k_1 = 1$, $k_2 = 1$, $c = 0.15$, $X_{init} = 100$. Network size: 100×100.

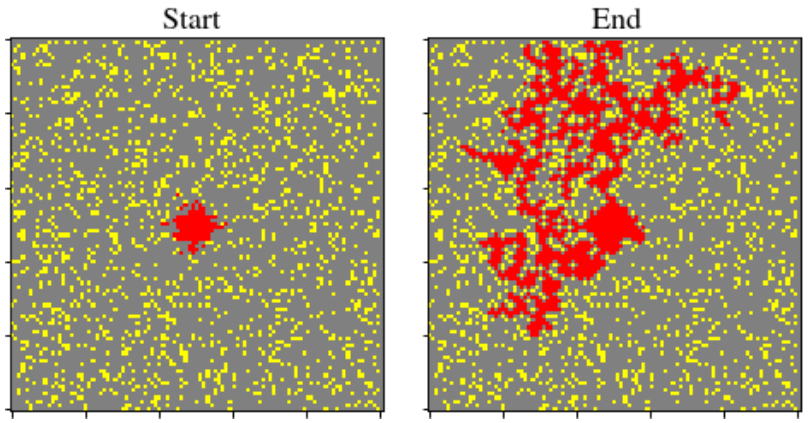

(a)

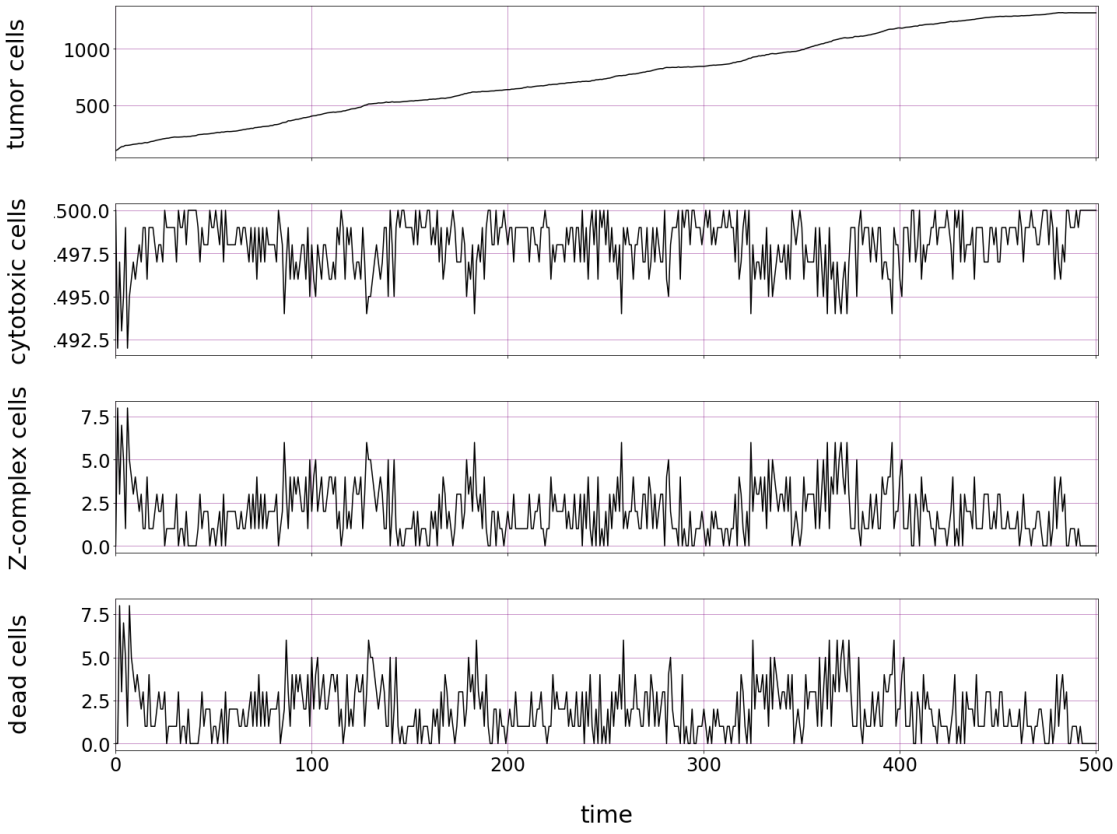

(b)

Figure 11.2: The evolution of the tumor that results in tumor full development in a lattice model a) initial state (left) versus state after $n = 500$ iterations (right), b) changes in concentration of tumor, cytotoxic, Z-complex and dead cells as a function of time. Simulation parameters: $\lambda = 0.3$, $k_1 = 1$, $k_2 = 1$, $c = 0.15$, $X_{init} = 100$. Network size: 100×100.

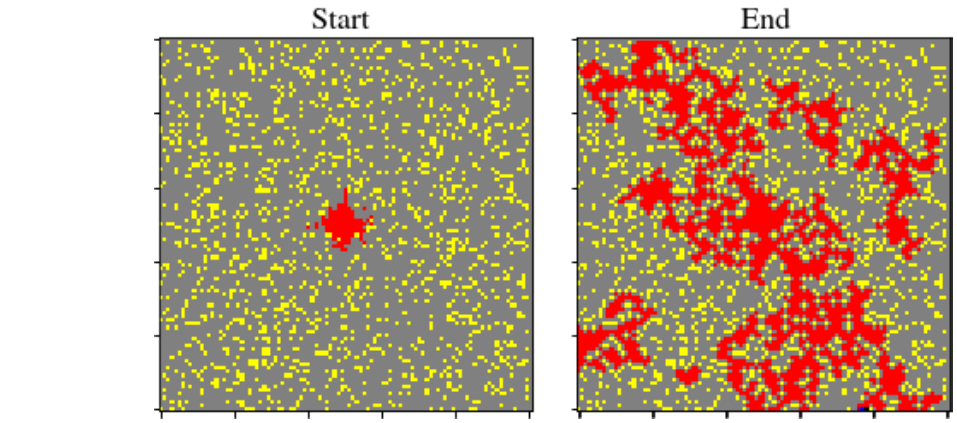

(a)

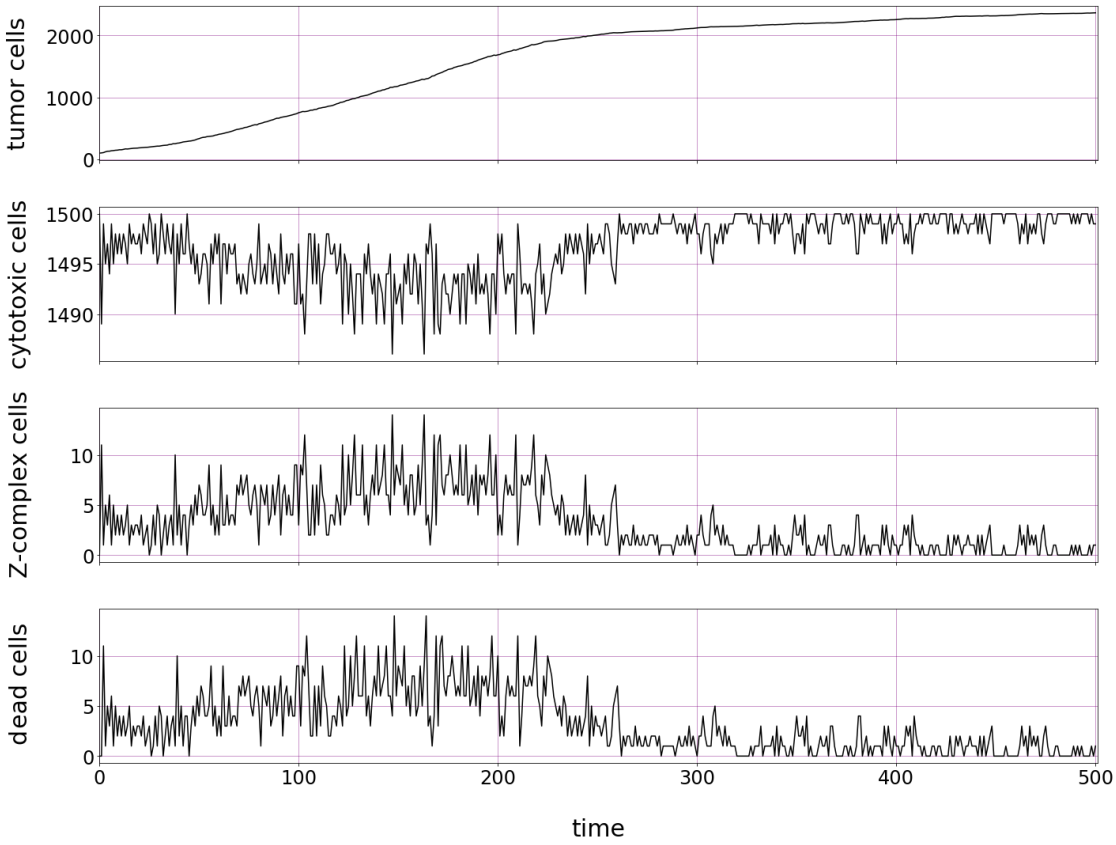

(b)

Figure 11.3: The evolution of the cancer in a small world network: a) initial state versus state after $n = 500$ iterations, b) changes in concentration of tumor, cytotoxic, Z-complex and dead cells as a function of time. Simulation parameters: $\lambda = 0.3$, $k_1 = 1$, $k_2 = 1$, $c = 0.15$, $X_{init} = 100$. Number of long range links: $n_{links} = 50$. Network size: 100×100.

Appendix B: Tables

Table 11.1:

The percentage of the sample networks where tumor cells reach the given range $r = \{20, 30, 40, 50\}$. The number of sample networks in the testing set: $k = 100$. The initial number of tumor cells: $X_{init} = 50$, number of long range links in the system: $n_{links} = 0$.

		20	**30**	**40**	**50**
c = 0.10	$\lambda = 0.3$	1.0	1.0	1.00	1.0
	$\lambda = 1.0$	1.0	1.0	1.00	1.0
c = 0.15	$\lambda = 0.3$	0.83	0.64	0.51	0.36
	$\lambda = 1.0$	1.0	1.0	1.0	1.0
c = 0.20	$\lambda = 0.3$	0.16	0.02	0.01	0.0
	$\lambda = 1.0$	0.97	0.89	0.84	0.80

Table 11.2:

The percentage of the sample networks where tumor cells reach the given range $r = \{20, 30, 40, 50\}$. The number of sample networks in the testing set: $k = 100$. The initial number of tumor cells: $X_{init} = 100$, number of long range links in the system: $n_{links} = 0$.

		20	**30**	**40**	**50**
c = 0.10	$\lambda = 0.3$	1.0	1.0	1.0	1.0
	$\lambda = 1.0$	1.0	1.0	1.0	1.0
c = 0.15	$\lambda = 0.3$	0.93	0.82	0.62	0.42
	$\lambda = 1.0$	1.0	1.0	1.0	1.0
c = 0.20	$\lambda = 0.3$	0.38	0.07	0.0	0.0
	$\lambda = 1.0$	0.99	0.97	0.94	0.90

Table 11.3:

The percentage of the sample networks where tumor cells reach the given range $r = \{20, 30, 40, 50\}$. The number of sample networks in the testing set: $k = 200$. The initial number of tumor cells: $X_{init} = 50$, number of long range links in the system: $n_{links} = 25$.

		20	**30**	**40**	**50**
c = 0.10	$\lambda = 0.3$	1.0	0.995	0.995	0.975
	$\lambda = 1.0$	1.0	1.0	1.0	1.0
c = 0.15	$\lambda = 0.3$	0.895	0.86	0.83	0.75
	$\lambda = 1.0$	1.0	1.0	1.0	1.0
c = 0.20	$\lambda = 0.3$	0.645	0.56	0.46	0.25
	$\lambda = 1.0$	0.995	0.98	0.97	0.97

Table 11.4:

The percentage of the sample networks where tumor cells reach the given range $r = \{20, 30, 40, 50\}$. The number of sample networks in the testing set: $k = 200$. The initial number of tumor cells: $X_{init} = 100$, number of long range links in the system: $n_{links} = 25$.

		20	**30**	**40**	**50**
c = 0.10	$\lambda = 0.3$	1.0	1.0	1.0	1.0
	$\lambda = 1.0$	1.0	1.0	1.0	1.0
c = 0.15	$\lambda = 0.3$	0.915	0.86	0.825	0.73
	$\lambda = 1.0$	1.0	1.0	1.0	1.0
c = 0.20	$\lambda = 0.3$	0.815	0.78	0.555	0.35
	$\lambda = 1.0$	1.0	1.0	1.0	1.0

Table 11.5:

The percentage of the sample networks where tumor cells reach the given range $r = \{20, 30, 40, 50\}$. The number of sample networks in the testing set: $k = 200$. The initial number of tumor cells: $X_{init} = 50$, number of long range links in the system: $n_{links} = 50$.

		20	**30**	**40**	**50**
c = 0.10	$\lambda = 0.3$	1.0	1.0	1.0	1.0
	$\lambda = 1.0$	1.0	1.0	1.0	1.0
c = 0.15	$\lambda = 0.3$	0.97	0.97	0.95	0.905
	$\lambda = 1.0$	1.0	1.0	1.0	1.0
c = 0.20	$\lambda = 0.3$	0.765	0.70	0.61	0.41
	$\lambda = 1.0$	1.0	1.0	1.0	0.99

Table 11.6:

The percentage of the sample networks where tumor cells reach the given range $r = \{20, 30, 40, 50\}$. The number of sample networks in the testing set: $k = 200$. The initial number of tumor cells: $X_{init} = 100$, number of long range links in the system: $n_{links} = 50$.

		20	**30**	**40**	**50**
c = 0.10	$\lambda = 0.3$	1.0	1.0	1.0	1.0
	$\lambda = 1.0$	1.0	1.0	1.0	1.0
c = 0.15	$\lambda = 0.3$	0.995	0.99	0.97	0.955
	$\lambda = 1.0$	1.0	1.0	1.0	1.0
c = 0.20	$\lambda = 0.3$	0.96	0.935	0.88	0.655
	$\lambda = 1.0$	1.0	1.0	0.995	0.99

Table 11.7:

The percentage of the sample networks where tumor cells reach the given range $r = \{20, 30, 40, 50\}$. The number of sample networks in the testing set: $k = 200$. The initial number of tumor cells: $X_{init} = 50$, number of long range links in the system: $n_{links} = 100$.

		20	**30**	**40**	**50**
c = 0.10	$\lambda = 0.3$	1.0	1.0	1.0	0.98
	$\lambda = 1.0$	1.0	1.0	1.0	1.0
c = 0.15	$\lambda = 0.3$	1.0	1.0	0.99	0.965
	$\lambda = 1.0$	0.995	0.995	0.995	0.995
c = 0.20	$\lambda = 0.3$	0.84	0.765	0.725	0.535
	$\lambda = 1.0$	1.0	1.0	0.995	0.99

Table 11.8:

The percentage of the sample networks where tumor cells reach the given range $r = \{20, 30, 40, 50\}$. The number of sample networks in the testing set: $k = 200$. The initial number of tumor cells: $X_{init} = 50$, number of long range links in the system: $n_{links} = 100$.

		20	**30**	**40**	**50**
c = 0.10	$\lambda = 0.3$	1.0	1.0	1.0	1.0
	$\lambda = 1.0$	1.0	1.0	0.995	0.995
c = 0.15	$\lambda = 0.3$	1.0	1.0	1.0	0.995
	$\lambda = 1.0$	1.0	1.0	1.0	1.0
c = 0.20	$\lambda = 0.3$	0.915	0.86	0.82	0.695
	$\lambda = 1.0$	1.0	1.0	1.0	1.0

Table 11.9:

The percentage of the sample networks where tumor cells reach the given range $r = \{20, 30, 40, 50\}$. The number of sample networks in the testing set: $k = 200$. The initial number of tumor cells: $X_{init} = 50$, number of long range links in the system: $n_{links} = 200$.

		20	**30**	**40**	**50**
c = 0.10	$\lambda = 0.3$	1.0	1.0	1.0	1.0
	$\lambda = 1.0$	1.0	1.0	1.0	1.0
c = 0.15	$\lambda = 0.3$	1.0	1.0	0.995	0.995
	$\lambda = 1.0$	1.0	1.0	1.0	1.0
c = 0.20	$\lambda = 0.3$	0.995	0.975	0.955	0.86
	$\lambda = 1.0$	1.0	1.0	1.0	1.0

Table 11.10:

The percentage of the sample networks where tumor cells reach the given range $r = \{20, 30, 40, 50\}$. The number of sample networks in the testing set: $k = 200$. The initial number of tumor cells: $X_{init} = 100$, number of long range links in the system: $n_{links} = 200$.

		20	**30**	**40**	**50**
c = 0.10	$\lambda = 0.3$	1.0	1.0	1.0	1.0
	$\lambda = 1.0$	1.0	1.0	1.0	1.0
c = 0.15	$\lambda = 0.3$	1.0	1.0	0.995	0.995
	$\lambda = 1.0$	1.0	1.0	1.0	1.0
c = 0.20	$\lambda = 0.3$	1.0	1.0	0.995	0.955
	$\lambda = 1.0$	1.0	1.0	1.0	1.0